



## The decay pattern of the Pygmy Dipole Resonance of $^{140}\text{Ce}$



B. Löher<sup>a,c,h,\*</sup>, D. Savran<sup>a,c</sup>, T. Aumann<sup>h,f</sup>, J. Beller<sup>h</sup>, M. Bhike<sup>b</sup>, N. Cooper<sup>i</sup>, V. Derya<sup>g</sup>, M. Duchêne<sup>h</sup>, J. Endres<sup>g</sup>, A. Hennig<sup>g</sup>, P. Humby<sup>i</sup>, J. Isaak<sup>a,c</sup>, J.H. Kelley<sup>e</sup>, M. Knörzer<sup>h</sup>, N. Pietralla<sup>h</sup>, V.Yu. Ponomarev<sup>h</sup>, C. Romig<sup>h</sup>, M. Scheck<sup>j,k</sup>, H. Scheit<sup>h</sup>, J. Silva<sup>a,c</sup>, A.P. Tonchev<sup>d</sup>, W. Tornow<sup>b</sup>, F. Wamers<sup>a,c,f</sup>, H. Weller<sup>b</sup>, V. Werner<sup>h,i</sup>, A. Zilges<sup>g</sup>

<sup>a</sup> ExtreMe Matter Institute EMMI and Research Division, GSI Helmholtzzentrum für Schwerionenforschung, Planckstr. 1, 64291 Darmstadt, Germany

<sup>b</sup> Department of Physics, Duke University and Triangle Universities Nuclear Laboratory, Durham, NC 27708-0308, USA

<sup>c</sup> Frankfurt Institute for Advanced Studies FIAS, Ruth-Moufang-Str. 1, 60438 Frankfurt am Main, Germany

<sup>d</sup> Physics Division, Lawrence Livermore National Laboratory, Livermore, CA 94551, USA

<sup>e</sup> Department of Physics, North Carolina State University, Raleigh, NC 27607, USA

<sup>f</sup> GSI Helmholtzzentrum für Schwerionenforschung, Planckstr. 1, 64291 Darmstadt, Germany

<sup>g</sup> Institut für Kernphysik, Universität zu Köln, Zùlpicher Str. 77, D-50937 Köln, Germany

<sup>h</sup> Institut für Kernphysik, TU Darmstadt, Schlossgartenstr. 9, 64289 Darmstadt, Germany

<sup>i</sup> WNSL, Yale University, P.O. Box 208120, New Haven, CT 06520-8120, USA

<sup>j</sup> University of the West of Scotland, Paisley PA1 2BE, UK

<sup>k</sup> SUPA, Scottish Universities Physics Alliance, Glasgow G12 8QQ, UK

### ARTICLE INFO

#### Article history:

Received 4 January 2016

Received in revised form 16 February 2016

Accepted 19 February 2016

Available online 23 February 2016

Editor: V. Metag

#### Keywords:

$\gamma$ -ray spectroscopy

$^{140}\text{Ce}$

Pygmy Dipole Resonance

Nuclear resonance fluorescence

Coincidence measurement

Quasi-particle phonon model

### ABSTRACT

The decay properties of the Pygmy Dipole Resonance (PDR) have been investigated in the semi-magic  $N = 82$  nucleus  $^{140}\text{Ce}$  using a novel combination of nuclear resonance fluorescence and  $\gamma$ - $\gamma$  coincidence techniques. Branching ratios for transitions to low-lying excited states are determined in a direct and model-independent way both for individual excited states and for excitation energy intervals. Comparison of the experimental results to microscopic calculations in the quasi-particle phonon model exhibits an excellent agreement, supporting the observation that the Pygmy Dipole Resonance couples to the ground state as well as to low-lying excited states. A 10% mixing of the PDR and the  $[2_1^+ \times \text{PDR}]$  is extracted.

© 2016 The Authors. Published by Elsevier B.V. This is an open access article under the CC BY license (<http://creativecommons.org/licenses/by/4.0/>). Funded by SCOAP<sup>3</sup>.

During the past 15 years, substructures of the E1 strength on top of the low-energy tail of the isovector Giant Dipole Resonance (IVGDR) [1] have been intensively studied. They are often referred to as the Pygmy Dipole Resonance (PDR); see [2] for a recent review. The location, total strength, as well as its fragmentation have been experimentally obtained for many stable (see Refs. [3–13]) and a few exotic neutron rich [14–17] nuclei along the nuclear chart. These studies were accompanied by theoretical efforts to describe this new phenomenon [18]. The ability to accurately describe the properties of the PDR is a delicate test for

modern nuclear models. In addition, the PDR and in general the electric dipole (E1) strength (via the dipole polarizability) have been shown to be connected to the neutron-skin thickness, and hence they are related to isovector parameters in the equation of state of nuclear matter [19–23].

In stable nuclei the PDR can be studied in detail using several experimental methods. The method of nuclear resonance fluorescence (NRF) is sensitive to  $J = 1$  states in even–even nuclei with high selectivity and allows to systematically study the fine structure of the PDR up to the particle separation thresholds [24–26]. Several important aspects regarding the nature of the PDR, such as collectivity, isospin character and interplay between these properties are currently being investigated using different theoretical approaches [18,21,27–31] providing controversial conclusions. Clearly, a solid and extensive experimental database is mandatory in order to discriminate and evaluate the different models.

\* Corresponding author at: GSI Helmholtzzentrum für Schwerionenforschung, Planckstr. 1, 64291 Darmstadt, Germany. Tel.: +49 6159713272; fax: +49 6159713475.

E-mail address: [b.loeher@gsi.de](mailto:b.loeher@gsi.de) (B. Löher).

In particular, experiments using a variety of probes, or providing additional complementary observables, are of high interest to test various aspects of the calculations. Excellent examples are recent experiments using the  $(\alpha, \alpha'\gamma)$  reaction at intermediate energy, which have revealed a structural splitting of the low-energy E1 strength for a number of different nuclei [32–36]. Measurements using inelastic scattering of  $^{17}\text{O}$  strongly support these results [37–39].

Here, we present the investigation of a new property of the PDR: probing its decay pattern by studying its direct decay to low-lying excited states. Such data provide additional insight into the nature of the decay mechanism of the PDR and pose a new challenge for nuclear theory. The role of many complex 2p2h and 3p3h configurations in the fragmentation of the 1p1h doorway  $1^-$  states has been already studied via ground-state transitions, and good agreement to data has been reported [7,11]. The investigation of direct decays of the PDR to low-lying states allows to draw conclusions on how some particular 2p2h configurations, namely the PDR built on top of these low-lying states, are mixed with the PDR itself. However, the direct observation of transitions to excited states is challenging, since experiments have shown that branching ratios  $\Gamma_i/\Gamma$  to states other than the ground state are small in comparison to the decay to the ground state. Therefore, most experiments were limited by their experimental sensitivity to the observation of direct decays to the ground state, and only indirect measurements of the decay pattern via the decay of low-lying states [9,40–44] were possible. Recently, the ratio of intensity from ground state transitions to the intensity for all transitions has been deduced from singles spectra measured at HI $\gamma$ S, representing comparable previous work [45]. A recent alternative approach to determine  $\Gamma_0/\Gamma$  using nuclear self-absorption suffered from low sensitivity to weakly excited states [46]. In this letter we report on the first direct determination of the branching intensity of the PDR to excited states using a novel experimental technique. Our results support the suggestion that the decay of PDR states is not the inverse reaction to its excitation by photons. Instead, while statistical decays dominate the high-energy part of the PDR, the direct decays to low-lying states strongly depend on the nuclear structure and may play an important role for the low-energy part of the PDR.

In NRF experiments, the integrated cross section for the  $i$ -th decay channel is proportional to  $\Gamma_0\Gamma_i/\Gamma$ , with the decay width to the ground state  $\Gamma_0$ , the decay width to an excited state  $\Gamma_i$  and level width  $\Gamma$ . Without adequate knowledge of the branching ratio  $\Gamma_i/\Gamma$ ,  $B(E1)\uparrow$  excitation strengths are often determined under the assumption that decays to excited states are negligible (i.e.  $\Gamma_i \ll 1$  and  $\Gamma_0 \approx \Gamma$ ). This is an invalid assumption, potentially leading to incorrect results if the sum of the partial decay widths to excited states  $\sum \Gamma_i$  becomes comparable to  $\Gamma_0$ . The use of quasi-monochromatic photon beams [47] allowed experiments with increased sensitivity compared to experiments using continuous-energy bremsstrahlung beams. Yet, the sensitivity for the direct observation of transitions to low-lying excited states has remained insufficient.

We report on the first results of experiments using the new approach of combining the high spin-selectivity of the NRF reaction to  $J = 1$  states, the benefit of quasi-monochromatic photon beams to excite the nucleus to states in a well defined energy region, and the high sensitivity to cascading transitions via  $\gamma$ - $\gamma$  coincidences in the decay radiation spectroscopy. The results are compared to calculations in the quasi-particle phonon model (QPM) [48], which accurately describes the bulk properties as well as the fragmentation of E1 strength in the PDR region [3,11]. The model has been extended to calculate the decay width of the PDR states to the first low-lying excited states of the nucleus.

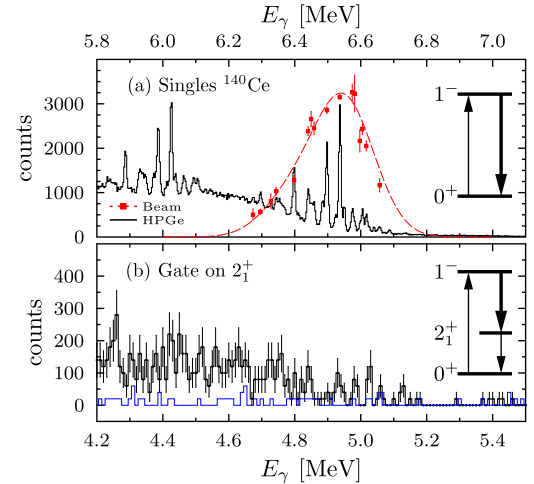


**Fig. 1.** (Color online.) Measured energy spectra for  $^{140}\text{Ce}$  at a beam energy of 6.5 MeV with simplified level schemes indicating the transitions visible in the spectrum (bold arrows). (a) Singles spectrum from HPGe detectors shown in black together with the spectral distribution of the photon beam (red, dashed). Red squares indicate values for the photon-flux determination from isolated transitions with known cross sections. (b) Spectrum of  $\gamma$ -rays detected by the HPGe spectrometers in coincidence with observation of the  $2_1^+ \rightarrow 0_1^+$  transition (1.596 MeV) in the LaBr detector array (black). Error bars indicate the statistical uncertainty. The blue histogram represents the background. The increasing intensity toward lower energy as well as the peak structures at 511 keV below the photon beam energy is due to the detector response. This has not been corrected for in the shown spectra to preserve the high energy resolution.

The experiments were performed using the recently installed  $\gamma$ - $\gamma$  coincidence setup  $\gamma^3$  at the High Intensity  $\gamma$ -ray Source (HI $\gamma$ S) at the Triangle Universities Nuclear Laboratory. The experimental setup is described in detail in [49] and technical details concerning the analysis of the measurements are given in [50]. The  $\gamma^3$  setup is located 52 m downstream from the production point of the  $\gamma$ -rays from laser Compton backscattering. The beam was collimated to a diameter of 1.9 cm at the target position to provide an intensity of  $3 \times 10^7$   $\gamma$ /s with an energy spread of about 4%. The photon beam impinged on the  $^{140}\text{Ce}$  target (mass: 2.3 g, isotopic enrichment: 99.72%) located at the center of the  $\gamma^3$  detector array. The array consisted of four 60% HPGe detectors providing high energy resolution as well as four large-volume 7.62 cm  $\times$  7.62 cm LaBr $_3$ :Ce scintillators with superior detection efficiency. The count-rate capability of LaBr $_3$ :Ce (see e.g. [51–53]) allowed for a close detector geometry, leading to a total efficiency of 6% for the LaBr $_3$ :Ce and 1.5% for the HPGe array at 1.3 MeV, respectively. The energy region of the PDR was covered from 5.2 MeV to 8.3 MeV.

Fig. 1(a) shows as an example the measured spectrum at a beam energy of 6.5 MeV, as detected by the HPGe  $\gamma$ -ray spectrometers (black) without any coincidence condition. The red dashed curve indicates the spectral distribution of the incident photon beam measured with an in-beam HPGe detector. The HPGe spectrum shows distinct peaks in the energy region of the photon beam, each corresponding to the decay of an excited  $J^\pi = 1^-$  state to the ground state. Near 6 MeV the single-escape peaks are visible. In a previous NRF experiment [46] the excitation cross sections for the most prominent transitions have been measured. They are used in the present experiment to calculate the absolute photon intensity (as indicated in Fig. 1(a)), which in turn allows to determine cross sections for previously unresolved transitions.

Fig. 1(b) shows the summed HPGe spectrum of photons detected in coincidence with a 1.596 MeV photon from the  $2_1^+ \rightarrow 0_1^+$  transition of  $^{140}\text{Ce}$  and detected with the LaBr array. The peaks

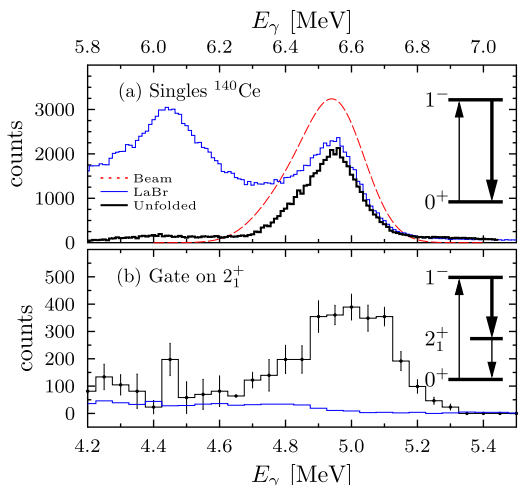


**Fig. 2.** (Color online.) Measured energy spectra from LaBr detectors. (a) Singles spectra from LaBr detectors (blue: measured, black: unfolded) together with the beam-energy distribution (red, dashed). (b) Coincidence spectrum (black) gated on the  $2_1^+ \rightarrow 0_1^+$  transition, unfolded using the fitting method. The small amount of random coincidences is shown in blue.

in this spectrum result from direct feeding transitions of the excited  $J = 1$  states at about 6.5 MeV into the first excited  $2_1^+$  state of  $^{140}\text{Ce}$ . From these feeding intensities the branching ratio to the  $2_1^+$  state relative to the ground state is determined. The spectrum resulting from a background gate on a slightly higher energy measured in the LaBr array is shown in blue, indicating the contribution of random coincidences. Clearly, the coincidence condition involving the decay of the  $2_1^+$  state is very selective and the spectrum is almost free of background. In addition, using the coincidence the transitions in the resulting spectrum can be unambiguously identified as primary transitions from the excited  $J = 1$  states. This demonstrates the high sensitivity of the employed method.

Complementing the state-to-state information extracted from the resolved peaks in the HPGe spectra, it is also possible to extract averaged quantities by integrating the energy spectra in the region of the excitation energy. In Fig. 2(a) the summed singles spectrum for the LaBr detectors is presented for the same incident photon beam energy of 6.5 MeV (blue histogram). Due to the energy resolution of the LaBr detectors of about 60 keV, it is not possible to observe single transitions. However, the enhanced detection efficiency provides superior statistics compared to the HPGe spectra. In order to analyse the full-energy peak, the spectrum is corrected for contributions from natural background radiation as well as effects of the detector response as described in [50]. The resulting spectrum is also shown in Fig. 2(a) in black. Fig. 2(b) shows the LaBr spectrum after unfolding (black) with the coincidence condition that one of the LaBr detectors has detected the 1.596 MeV photon from the  $2_1^+ \rightarrow 0_1^+$  transition. The blue histogram shows again the contribution of random coincidences and was produced in the same way as in Fig. 1(b) for the HPGe detectors. The same procedure of unfolding can also be applied to the HPGe spectra, yielding similar unfolding results. These, however, contain much less statistics compared to the unfolded LaBr spectra, due to the smaller detection efficiency of the HPGe detectors.

The area of the full-energy peak in the unfolded HPGe and LaBr spectra is composed of the summed areas of the full-energy peaks, which could be resolved in the HPGe spectra, and in addition contains also the aggregate area of all unresolved transitions. The ratio of the total scattering cross section  $\sigma_{\gamma\gamma}^I$  as determined from integrating the unfolded spectra, and the sum of the scattering cross

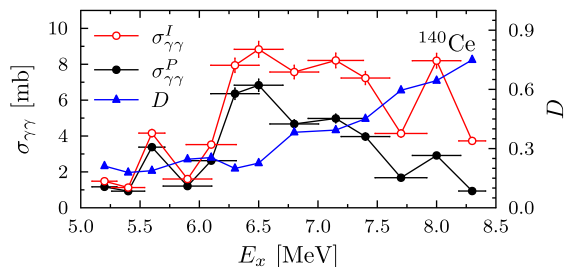


**Fig. 3.** (Color online.) Elastic scattering cross section of  $^{140}\text{Ce}$  extracted from HPGe spectra. Points shown as filled circles (black) consider solely integrated cross sections of observed individual ground-state transitions. Open circles (red) include also the contribution from unresolved states. The normalised difference between the two values  $D$  is shown with blue triangles. Horizontal error bars indicate the FWHM of the beam-energy distribution. Lines are drawn as a guide.

sections of the isolated states  $\sigma_{\gamma\gamma}^P$ , therefore provides a measure of the amount of unresolved strength missing in the state-to-state analysis. Fig. 3 compares both values extracted from HPGe spectra as a function of the excitation energy. For the determination of absolute cross sections the previously known values for strong transitions from [5] and [46] have been used to calibrate the photon flux. At energies below about 6.5 MeV most of the total scattering cross section can be resolved into isolated states within the HPGe resolution, while at higher energies the accumulated contribution of weakly excited levels to  $\sigma_{\gamma\gamma}^I$  can no longer be neglected. This trend is clearly visible from the normalised difference  $D = 1 - \sigma_{\gamma\gamma}^P / \sigma_{\gamma\gamma}^I$ .

Recently, a comparative study between NRF and  $(p, p')$  measurements [54] has shown a significant discrepancy regarding the total E1 strength. In light of this study it is important to precisely determine the cross section taking into account also the contribution from unresolved states as well as from transitions to low-lying excited states. The large value of  $D$  at higher energy indicates that the disagreement between the  $(p, p')$  and NRF results at these energies may partly be explained by contributions from unresolved ground state transitions. The determination of such unresolved transitions has been investigated also in NRF experiments before, for example on  $^{136}\text{Ba}$  and other nuclei, see [45,55] and references therein. In the analysis of these experiments the results were obtained by using Monte-Carlo simulations as well as statistical model calculations to account for background and contributions from inelastic transitions, which, however, introduce a model-dependency in the results. In addition to the contribution from unresolved transitions, the direct decay to low-lying states contributes significantly to the total cross section, even in an energy region with low level density, as is shown below.

When requiring a transition to a low-lying excited state in coincidence, a spectrum containing only the contributions from inelastic transitions is obtained, and therefore it is possible to extract the branching ratio to this excited state in a model-independent way. Compared to the coincident HPGe spectra the LaBr spectra contain much higher statistics. At the same time the LaBr spectra do not allow for a state-to-state analysis, but instead averaged branching ratios can be extracted from the data for the excitation energy region defined by the photon beam. The averaged branching ratio  $\langle b_i \rangle$  describes the fraction of decays to the  $2_1^+$  state relative to the ground state decays. It is connected to the branching ratios of single excited states by

$$\langle b_i \rangle = \sum_j \Gamma_0^j \frac{\Gamma_i^j}{\Gamma^j} / \sum_j \frac{(\Gamma_0^j)^2}{\Gamma^j}, \quad (1)$$

where the index  $j$  denotes the  $j$ -th  $J = 1$  excitation in the given excitation energy region, and the index  $i$  the  $i$ -th final state. The  $\langle b_i \rangle$  can be compared to the calculations within the QPM.

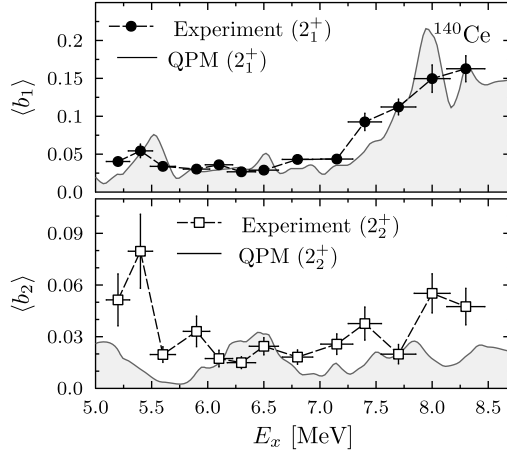


**Fig. 4.** Averaged branching ratio  $\langle b_i \rangle$  to excited states for  $^{140}\text{Ce}$  as a function of excitation energy  $E_x$  compared to results from QPM calculation (solid curve). Circles: Transition to  $2_1^+$  state. Squares: Transition to  $2_2^+$  state. Error bars include statistical uncertainties, and systematical uncertainties owed to efficiency extrapolation and unfolding.

Fig. 4 shows the results for analysis of the LaBr coincidence spectra. In the upper part the average branching ratio  $\langle b_1 \rangle$  to the first excited  $2_1^+$  state of  $^{140}\text{Ce}$  is given as a function of excitation energy. The lower panel shows the average branching ratio  $\langle b_2 \rangle$  for the decay to the  $2_2^+$  state at an excitation energy of 2.348 MeV.

The calculations shown in the upper part of Fig. 4 were already performed during the planning stage of the experiment to estimate the feasibility of this type of experiment. The wave functions of the PDR states of  $^{140}\text{Ce}$  were taken from previous calculations presented in [11]. They contain one-, two-, and three-phonon components:

$$|\Psi_\lambda\rangle_\nu = \left\{ \sum_{\lambda i} R_{\lambda i}^\nu Q_{\lambda i}^\dagger + \sum_{\lambda' i' \lambda'' i''} P_{\lambda' i' \lambda'' i''}^\nu(v) \left[ Q_{\lambda' i'}^\dagger \times Q_{\lambda'' i''}^\dagger \right]_\lambda \right. \\ \left. + \sum_{\lambda' i' \lambda'' i''} \sum_{\lambda''' i''' j'} T_{\lambda' i' \lambda'' i'' \lambda''' i''' j'}^\nu(v) \left[ \left[ Q_{\lambda' i'}^\dagger \times Q_{\lambda'' i''}^\dagger \right]_{j'} \times Q_{\lambda''' i'''}^\dagger \right]_\lambda \right\} | \rangle_{\text{g.s.}} \quad (2)$$

where  $Q_{\lambda i}^\dagger$  is a phonon of the multipolarity  $\lambda = J^\pi$  and root number  $i$  of the quasi-particle random phase approximation;  $[Q_{\lambda' i'}^\dagger \times Q_{\lambda'' i''}^\dagger]_\lambda = \sum_{m' m''} C_{\lambda' m' \lambda'' m''}^{\lambda m} Q_{\lambda' m'}^\dagger Q_{\lambda'' m''}^\dagger$ . The amplitudes of one-, two-, and three-phonon configurations into a  $\nu$ -th mixed state are denoted by  $R$ ,  $P$ , and  $T$ , respectively.

The wave functions of the  $2_{\nu_2}^+$  ( $\nu_2 = 1, 2$ ) states are dominated by one-phonon components (see Table II(b) in [56]). The decay widths of the  $1_{\nu_1}^-$  ( $\nu_1 = 1, 2, \dots$ ) state to the ground state  $\Gamma_0(1_{\nu_1}^- \rightarrow \text{g.s.}) \propto B(E1, \text{g.s.} \rightarrow 1_{\nu_1}^-)$  are calculated from the results in [11]. The decay widths to the excited  $2_{\nu_2}^+$  state have the form

$$\Gamma_{2_{\nu_2}^+}(1_{\nu_1}^- \rightarrow 2_{\nu_2}^+) \propto \left| \sum_{i_2} R_{i_2}^{\nu_1} \left( \sum_{i_1} R_{i_1}^{\nu_1} \langle Q_{2+i_2} \| E1 \| Q_{1-i_1}^+ \rangle \right. \right. \\ \left. \left. + \sum_{\lambda_1 i \lambda_2 i'} P_{\lambda_1 i \lambda_2 i'}^{\lambda_2 i'}(\nu_1) \langle Q_{2+i_2} \| E1 \| [Q_{\lambda_1 i}^+ Q_{\lambda_2 i'}^+]_{1-} \rangle \right) \right|^2, \quad (3)$$

where E1 means the electric dipole transition operator. Index 1 or 2 in Eq. (3) refers to specific multipolarity  $1^-$  or  $2^+$ , respectively. Expressions for reduced matrix elements are available in [57].

Among the many transition matrix elements in Eq. (3) only a few of them provide the main contribution to the final sum. They are  $\langle Q_{2+i_2} \| E1 \| [Q_{1-i_1}^+ Q_{2+i_2}^+]_{1-} \rangle$ , representing the decay of the doorway PDR states built on top of the  $2_{\nu_2}^+$  low-lying state. The sum of all other matrix elements contributes only about 15% on average to the  $\Gamma_{2_{\nu_2}^+}$ . At the same time, the excitation probability of the  $1_{\nu_1}^-$  states and their decay width to the ground state are proportional, with good accuracy, to the excitation probability of the doorway PDR states. This allows for a sensitive test of the mixing of the PDR and the PDR built on top of the  $2_{\nu_2}^+$  low-lying states. The discrete branching ratios obtained from the QPM calculation have been averaged using a Lorentz-shape distribution with a width corresponding to the energy spread of the photon beam (from about 200 keV to 400 keV). The resulting averaged branching ratio as a function of the excitation energy is shown as a solid curve in Fig. 4.

Comparison of the experimental data to the results from the QPM calculation reveals very good agreement, both, in terms of the absolute value and the energy dependence over the entire energy range. In case of the decay to the  $2_2^+$  state the agreement is not as good as for the  $2_1^+$  state. The reason may be that the strength of the quadrupole residual interaction in the model Hamiltonian has been adjusted to describe the properties of the first  $2^+$  state as accurately as possible. Yet, this is a clear indication that the coupling to complex configurations in the QPM leads not only to an adequate description of the strength fragmentation, but in addition describes the transition probabilities to excited states with good accuracy. In particular, the determination of the branching intensity to the first excited states provides a sensitive test on how the PDR and the PDR built on top of these low-lying excited states are mixed.

These studies finally allow for the determination of the magnitude of the mixing between the PDR and the PDR built on top of low-lying states, which is assumed weak by the Axel–Brink hypothesis. We conclude that in  $^{140}\text{Ce}$  the PDR and  $[2_1^+ \times \text{PDR}]$  are mixed on the level of about 10%, while this mixing is weaker for the  $[2_2^+ \times \text{PDR}]$  mode.<sup>1</sup>

In summary, we presented for the first time a direct determination of decay properties of the PDR using a novel experimental approach, which combines a quasi-monochromatic photon beam and  $\gamma$ - $\gamma$ -coincidence spectroscopy. This approach, applied to  $^{140}\text{Ce}$ , provides the necessary sensitivity to directly observe decays to excited states of the nucleus. The experimental method allowed for the determination of the contribution from unresolved transitions to the measured cross sections. The averaged branching ratios to the first and second excited  $2^+$  states were measured, even though the absolute values are only a few percent, which demonstrates the superior sensitivity of the method. The QPM has been extended to provide transition widths to low lying excited states. The model prediction for the decay to the first excited  $2^+$  state is in a very good agreement with the new data. The results from these measurements are also important for NRF studies in general, and hint at the necessity of corrections to already measured PDR excitation cross sections.

The work described in this article is supported by the Alliance Program of the Helmholtz Association (HA216/EMMI), the DFG (SFB 1245 and Z1510/7-1) and U.S. DOE grants No. DE-FG02-91ER-40609 and No. DE-FG02-97ER-41033.

<sup>1</sup> It should be noted, that the so-called statistical decay is very different from what we observe here, because the strength of the mixing is tied to the collectivity of the participating  $2^+$  state, which is a property of nuclear structure.

## References

- [1] M.N. Harakeh, A. Woude, *Giant Resonances: Fundamental High-Frequency Modes of Nuclear Excitation*, vol. 24, Oxford University Press, 2001.
- [2] D. Savran, T. Aumann, A. Zilges, *Prog. Part. Nucl. Phys.* 70 (2013) 210.
- [3] R.-D. Herzberg, P. von Brentano, J. Eberth, J. Enders, R. Fischer, N. Huxel, T. Klemme, P. von Neumann-Cosel, N. Nicolay, N. Pietralla, et al., *Phys. Lett. B* 390 (1997) 49.
- [4] K. Govaert, F. Bauwens, J. Bryssinck, D. De Frenne, E. Jacobs, W. Mondelaers, L. Govor, V.Y. Ponomarev, *Phys. Rev. C* 57 (1998) 2229.
- [5] A. Zilges, S. Volz, M. Babilon, T. Hartmann, P. Mohr, K. Vogt, *Phys. Lett. B* 542 (2002) 43.
- [6] T. Hartmann, M. Babilon, S. Kamedzhiev, E. Litvinova, D. Savran, S. Volz, A. Zilges, *Phys. Rev. Lett.* 93 (2004) 192501.
- [7] D. Savran, M. Fritzsche, J. Hasper, K. Lindenberg, S. Müller, V. Ponomarev, K. Sonnabend, A. Zilges, *Phys. Rev. Lett.* 100 (2008).
- [8] R. Schwengner, G. Rusev, N. Tsoneva, N. Benouaret, R. Beyer, M. Erhard, E. Grosse, A. Junghans, J. Klug, K. Kosev, et al., *Phys. Rev. C* 78 (2008) 064314.
- [9] A.P. Tonchev, S.L. Hammond, J.H. Kelley, E. Kwan, H. Lenske, G. Rusev, W. Tornow, N. Tsoneva, *Phys. Rev. Lett.* 104 (2010) 072501.
- [10] A. Tamii, I. Poltoratska, P. Von Neumann-Cosel, Y. Fujita, T. Adachi, C.A. Bertulani, J. Carter, M. Dozono, H. Fujita, K. Fujita, et al., *Phys. Rev. Lett.* 107 (2011) 062502.
- [11] D. Savran, M. Elvers, J. Endres, M. Fritzsche, B. Löher, N. Pietralla, V.Y. Ponomarev, C. Romig, L. Schnorrenberger, K. Sonnabend, et al., *Phys. Rev. C* 84 (2011) 024326.
- [12] J. Isaak, D. Savran, M. Fritzsche, D. Galaviz, T. Hartmann, S. Kamedzhiev, J.H. Kelley, E. Kwan, N. Pietralla, C. Romig, et al., *Phys. Rev. C* 83 (2011) 034304.
- [13] R. Schwengner, R. Massarczyk, G. Rusev, N. Tsoneva, D. Bemmerer, R. Beyer, R. Hannaske, A.R. Junghans, J.H. Kelley, E. Kwan, et al., *Phys. Rev. C* 87 (2013) 024306.
- [14] P. Adrich, A. Klimkiewicz, M. Fallot, K. Boretzky, T. Aumann, D. Cortina-Gil, U. Pramank, T. Elze, H. Emling, H. Geissel, et al., *Phys. Rev. Lett.* 95 (2005) 132501.
- [15] J. Gibelin, D. Beaumel, T. Motobayashi, Y. Blumenfeld, N. Aoi, H. Baba, Z. Elekes, S. Fortier, N. Frascaria, N. Fukuda, et al., *Phys. Rev. Lett.* 101 (2008) 212503.
- [16] O. Wieland, A. Bracco, *Prog. Part. Nucl. Phys.* 66 (2011) 374.
- [17] D.M. Rossi, P. Adrich, F. Aksouh, H. Alvarez-Pol, T. Aumann, J. Benlliure, M. Böhmer, K. Boretzky, E. Casarejos, M. Chartier, et al., *Phys. Rev. Lett.* 111 (2013) 242503.
- [18] N. Paar, D. Vretenar, E. Khan, G. Colo, *Rep. Prog. Phys.* 70 (2007) 691.
- [19] P.-G. Reinhard, W. Nazarewicz, *Phys. Rev. C* 81 (2010) 051303.
- [20] J. Piekarewicz, B.K. Agrawal, G. Colò, W. Nazarewicz, N. Paar, P.-G. Reinhard, X. Roca-Maza, D. Vretenar, *Phys. Rev. C* 85 (2012) 041302.
- [21] X. Roca-Maza, G. Pozzi, M. Brenna, K. Mizuyama, G. Colò, *Phys. Rev. C* 85 (2012) 024601.
- [22] X. Roca-Maza, M. Brenna, G. Colò, M. Centelles, X. Viñas, B.K. Agrawal, N. Paar, D. Vretenar, J. Piekarewicz, *Phys. Rev. C* 88 (2013) 024316.
- [23] N. Paar, A. Horvat, *EPJ Web Conf.* 66 (2014) 02078.
- [24] U. Kneissl, H. Pitz, A. Zilges, *Prog. Part. Nucl. Phys.* 37 (1996) 349.
- [25] U. Kneissl, N. Pietralla, A. Zilges, *J. Phys. G* 32 (2006) R217.
- [26] N. Tsoneva, H. Lenske, *Phys. Rev. C* 77 (2008) 024321.
- [27] N. Paar, Y.F. Niu, D. Vretenar, J. Meng, *Phys. Rev. Lett.* 103 (2009) 032502.
- [28] E. Litvinova, P. Ring, V. Tselyaev, *Phys. Rev. Lett.* 105 (2010) 022502.
- [29] P. Papakonstantinou, H. Hergert, V. Ponomarev, R. Roth, *Phys. Lett. B* 709 (2012) 270.
- [30] D. Vretenar, Y.F. Niu, N. Paar, J. Meng, *Phys. Rev. C* 85 (2012) 044317.
- [31] E.G. Lanza, A. Vitturi, E. Litvinova, D. Savran, *Phys. Rev. C* 89 (2014) 041601.
- [32] D. Savran, M. Babilon, A.M. van den Berg, M.N. Harakeh, J. Hasper, A. Matic, H.J. Wörtche, A. Zilges, *Phys. Rev. Lett.* 97 (2006) 172502.
- [33] J. Endres, D. Savran, A.M. van den Berg, P. Dendooven, M. Fritzsche, M.N. Harakeh, J. Hasper, H.J. Wörtche, A. Zilges, *Phys. Rev. C* 80 (2009) 034302.
- [34] J. Endres, E. Litvinova, D. Savran, P. Butler, M. Harakeh, S. Harissopoulos, R.-D. Herzberg, R. Krücken, A. Lagoyannis, N. Pietralla, et al., *Phys. Rev. Lett.* 105 (2010) 212503.
- [35] V. Derya, J. Endres, M.N. Harakeh, D. Savran, H.J. Wörtche, A. Zilges, *J. Phys. Conf. Ser.* 366 (2012) 012012.
- [36] V. Derya, J. Endres, M. Elvers, M. Harakeh, N. Pietralla, C. Romig, D. Savran, M. Scheck, F. Siebenhühner, V. Stoica, et al., *Nucl. Phys.* 906 (2013) 94.
- [37] L. Pellegri, A. Bracco, F. Crespi, S. Leoni, F. Camera, E. Lanza, M. Kmiecik, A. Maj, R. Avigo, G. Benzoni, et al., *Phys. Lett. B* 738 (2014) 519.
- [38] F.C.L. Crespi, A. Bracco, R. Nicolini, D. Mengoni, L. Pellegri, E.G. Lanza, S. Leoni, A. Maj, M. Kmiecik, R. Avigo, et al., *Phys. Rev. Lett.* 113 (2014) 012501.
- [39] A. Bracco, F.C.L. Crespi, E.G. Lanza, *Eur. Phys. J. A* 51 (2015) 99.
- [40] C.T. Angell, S.L. Hammond, H.J. Karwowski, J.H. Kelley, M. Kr̕ička, E. Kwan, A. Makinaga, G. Rusev, *Phys. Rev. C* 86 (2012) 051302.
- [41] P.M. Goddard, N. Cooper, V. Werner, G. Rusev, P.D. Stevenson, A. Rios, C. Bernards, A. Chakraborty, B.P. Crider, J. Glorius, et al., *Phys. Rev. C* 88 (2013) 064308.
- [42] J. Isaak, D. Savran, M. Kr̕ička, M. Ahmed, J. Beller, E. Fiori, J. Glorius, J. Kelley, B. Löher, N. Pietralla, et al., *Phys. Lett. B* 727 (2013) 361.
- [43] C. Romig, J. Beller, J. Glorius, J. Isaak, J.H. Kelley, E. Kwan, N. Pietralla, V.Y. Ponomarev, A. Sauerwein, D. Savran, et al., *Phys. Rev. C* 88 (2013) 044331.
- [44] M. Scheck, V.Y. Ponomarev, T. Aumann, J. Beller, M. Fritzsche, J. Isaak, J.H. Kelley, E. Kwan, N. Pietralla, R. Raut, et al., *Phys. Rev. C* 87 (2013) 051304.
- [45] R. Massarczyk, R. Schwengner, F. Dönau, E. Litvinova, G. Rusev, R. Beyer, R. Hannaske, A.R. Junghans, M. Kempe, J.H. Kelley, et al., *Phys. Rev. C, Nucl. Phys.* 86 (2012) 014319.
- [46] C. Romig, D. Savran, J. Beller, J. Birkhan, A. Endres, M. Fritzsche, J. Glorius, J. Isaak, N. Pietralla, M. Scheck, et al., *Phys. Lett. B* 744 (2015) 044331.
- [47] H.R. Weller, M.W. Ahmed, H. Gao, W. Tornow, Y.K. Wu, M. Gai, R. Miskimen, *Prog. Part. Nucl. Phys.* 62 (2009) 257.
- [48] V.G. Soloviev, *Theory of Atomic Nuclei: Quasiparticles and Phonons*, Institute of Physics, Bristol, 1992.
- [49] B. Löher, V. Derya, T. Aumann, J. Beller, N. Cooper, M. Duchêne, J. Endres, E. Fiori, J. Isaak, J. Kelley, et al., *Nucl. Instrum. Methods Phys. Res., Sect. A, Accel. Spectrom. Detect. Assoc. Equip.* 723 (2013) 136.
- [50] B. Löher, Ph.D. thesis, Johannes Gutenberg-Universität, 2014, urn:nbn:de:hebis:77-38195.
- [51] B. Löher, D. Savran, E. Fiori, M. Miklavc, N. Pietralla, M. Vencelj, *Nucl. Instrum. Methods Phys. Res., Sect. A, Accel. Spectrom. Detect. Assoc. Equip.* 686 (2012) 1.
- [52] L. Stevanato, D. Cester, G. Nebbia, G. Viesti, F. Neri, S. Petrucci, S. Selmi, C. Tintori, *Nucl. Instrum. Methods Phys. Res., Sect. A, Accel. Spectrom. Detect. Assoc. Equip.* 678 (2012) 83.
- [53] M. Nocente, M. Tardocchi, A. Olariu, S. Olariu, R. Pereira, I. Chugunov, A. Fernandes, D. Gin, G. Grosso, V. Kiptily, et al., *IEEE Trans. Nucl. Sci.* 60 (2013) 1408.
- [54] A. Krumbholz, P. von Neumann-Cosel, T. Hashimoto, A. Tamii, T. Adachi, C. Bertulani, H. Fujita, Y. Fujita, E. Ganioglu, K. Hatanaka, et al., *Phys. Lett. B* 744 (2015) 7.
- [55] R. Massarczyk, G. Schramm, T. Belgia, R. Schwengner, R. Beyer, D. Bemmerer, Z. Elekes, E. Grosse, R. Hannaske, A.R. Junghans, et al., *Phys. Rev. C, Nucl. Phys.* 93 (2016) 014301.
- [56] W. Kim, B.L. Miller, J.R. Calarco, L.S. Cardman, J.P. Connelly, S.A. Fayans, B. Frois, D. Goutte, J.H. Heisenberg, F.W. Hersman, et al., *Phys. Rev. C* 45 (1992) 2290.
- [57] V.Y. Ponomarev, C. Stoyanov, N. Tsoneva, M. Grinberg, *Nucl. Phys.* 635 (1998) 470.